GEOPHYSICS, VOL. 75, NO. 6 (NOVEMBER-DECEMBER 2010); P. L91–L100, 14 FIGS., 1 TABLE.
10.1190/1.3494596

Application of the magnetic resonance sounding method to the investigation of aquifers in the presence of magnetic materials

Anatoly Legchenko[1], Jean-Michel Vouillamoz[1], and Jean Roy[2]

ABSTRACT

It has been previously reported that the magnetic resonance sounding (MRS) method does not produce reliable data in areas where magnetic rocks perturb the geomagnetic field. The applicability of the MRS can be extended by using the spin echo (SE) measuring technique instead of the commonly used measuring scheme based on recordings of the free induction decay (FID) signal. Modifications to the MRS method are presented for measuring and interpreting SE signals. Field results obtained in Cyprus (1999), Canada (2008), and India (2008) reveal that in test sites MRS measurements in the SE mode make it possible to apply the MRS method where the subsurface is composed of sand and gravel that contain magnetite or basalt and in aquifers composed of nonmagnetic sand overlying a magnetic basement. Considering the widespread occurrence of magnetic rocks, this development increases the area where MRS can be applied. However, experience shows that it is more time consuming to measure the SE and more complicated to interpret the field data than it is to work with FID measurements. Numerical results show that the MRS method in the SE mode is less efficient than the FID technique because of the smaller amplitude and wider band of the SE signal. Due to instrumental limitations and unknown distribution of the magnetic fields within the investigated volume, accuracy of the presented MRS-SE approach is site dependent. In a general case, MRS-SE in its current implementation is not able to provide robust estimates of the initial amplitude, which renders MRS estimate of the water content qualitative. For accurate estimate of the water content, more sophisticated approaches need to be developed.

INTRODUCTION

The magnetic resonance sounding (MRS) method is based on the nuclear magnetic resonance (NMR) phenomenon (Slichter, 1990). MRS is a selective method that is specifically sensitive to groundwater. MRS has the primary advantage of being able to directly detect subsurface water, as compared to other geophysical tools used for hydrogeological investigations. Currently available MRS instruments measure the free induction decay (FID) signal; however, it has been reported (Legchenko et al., 2002; Roy et al., 2008) that this method does not produce reliable data when the geomagnetic field is perturbed by magnetic rocks (for example, magnetite or basalt). For this reason, magnetic rock is considered one of the major limitations for the MRS method.

It is known that the spin echo (SE) technique that is widely used in laboratory NMR instruments and NMR logging tools can provide reliable results in the heterogeneous static magnetic field. In the presence of magnetic rocks, the geomagnetic field becomes nonhomogeneous and thus the idea of adapting the SE technique for MRS sounds promising. The very first MRS measurements in SE mode were performed in the early 1990s in Novosibirsk, Russia, thus demonstrating that the SE signal could be measured with MRS.

The spin echo is a more complicated phenomenon than a simple FID method. It requires at least two pulses, more power, and more accurate instrumental implementation. Magnetic rocks were originally considered a minor problem for MRS and thus the development of the SE technique was not the first priority for the MRS community. SE experiments were reported in the literature (Shushakov, 1996; Legchenko et al., 2002; Shushakov and Fomenko, 2004), but the SE technique was never used for systematic measurements.

With increasing MRS experience, it became apparent that magnetic rocks are common in many areas of the world and that this limited the use of MRS as a geophysical tool. To improve MRS performance, we adapted the well-known SE technique that had been developed especially for heterogeneous magnetic fields (Hahn, 1950)

Manuscript received by the Editor 25 June 2009; revised manuscript received 20 April 2010; published online 29 October 2010.
[1]IRD-LTHE, Grenoble, France. E-mail: anatoli.legtchenko@ird.fr; Jean-Michel.Vouillamoz@ird.fr.
[2]IGP, Outremont, Université Grenoble, Quebec, Canada. E-mail: jeanroy_igp@videotron.ca.

to MRS measurements. This adaptation consisted of developing a data acquisition program, a numerical modeling routine, and inversion software. For this first step, we did not modify the hardware of the MRS instrument. The SE technique and its field implementation were tested in areas where the geomagnetic field is known to be perturbed by magnetic materials in the subsurface: Cyprus (1999), the Grenville geological province (Canada, 2008), and Southern India (2008).

In this paper, we present a brief description of the method. For the interpretation of SE measurements, we developed a simplified mathematical model. Using this model, we numerically investigate the basic parameters of the method such as the depth of investigation and vertical resolution of MRS in SE mode and compare these to traditional MRS in FID mode. The field examples are used to demonstrate our experimental results.

BACKGROUND

MRS in the spin echo (SE) configuration

An MRS field set-up consists of a coincident transmitting/receiving loop laid out on the ground. The frequency of the MRS signal is equal to the Larmor frequency of the hydrogen protons in the geomagnetic field $f_0 = \omega_0/2\pi = \gamma B_0/2\pi$, where B_0 is the geomagnetic field and γ the gyromagnetic ratio of the protons. The loop is energized by a pulse of an alternating current $i(t) = I_0 \cos(\omega t)$ with the frequency $\omega \approx \omega_0$ that creates an alternating magnetic field in the subsurface. One sounding is composed of MRS signals measured for different values of the pulse moment $q = I_0\tau$, where I_0 and τ are the amplitude and duration of the pulse, respectively. The transverse component of the spin magnetization $M_\perp$ creates an alternating magnetic field that can be measured after the pulse cut-off. In an electrically conductive medium, the oscillating magnetic field $B_1(\mathbf{r})$ is elliptically polarized and can be represented by its co- and counterrotating components that generally are not equal (Weichman et al., 2000); however, the field $B_1(\mathbf{r})$ may also be approximated by a linearly polarized field. It has been shown that for a horizontally stratified subsurface, the error caused by this approximation is negligibly small (Valla and Legchenko, 2002; Legchenko et al., 2008). Assuming a linear polarization of the transmitted magnetic field, the induced signal in the receiving loop is represented by the following equation (Legchenko and Valla, 2002):

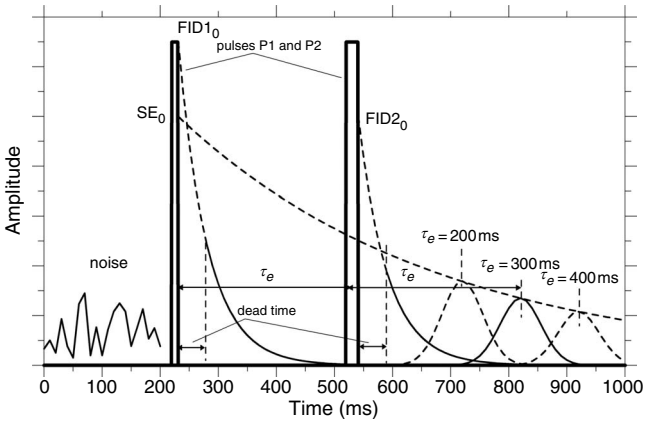

Figure 1. Typical time diagram of MRS measuring.

$$e_0(q) = \omega_0 \int_V \beta_1 \exp(j\varphi_0(\mathbf{r}))M_\perp(q,\mathbf{r})w(\mathbf{r})dV, \qquad (1)$$

where $\beta_1 = I_0^{-1}B_1$ is the normalized magnetic field created by the loop, $0 \le w(\mathbf{r}) \le 1$ is the water content, and $\mathbf{r} = r(x,y,z)$ is the coordinate vector.

The signal generated by the volume dV has a phase shift that is due to the electromagnetic shift caused by the electrical conductivity of the rocks

$$\varphi_0(\mathbf{r}) = 2\tan^{-1}(\mathrm{Im}(B_1)/\mathrm{Re}(B_1)). \qquad (2)$$

In a homogeneous geomagnetic field, $M_\perp$ can be measured by transmitting a single pulse and observing the free induction decay signal (FID1 in Figure 1). Under the exact resonance, $M_\perp$ thus becomes

$$M_\perp = M_0 \sin(\theta), \qquad (3)$$

where M_0 is the nuclear magnetization of the protons and $\theta = 0.5\gamma\beta_1 q$ is the flip angle.

In a nonhomogeneous geomagnetic field, the FID signal becomes short and can be difficult or impossible to measure. In this case, SE measurements can be used (Hahn, 1950). The measuring scheme (Figure 1) consists of transmitting two consecutive pulses separated by a time interval τ_e. The SE signal can be observed at time τ_e after the second pulse is terminated. For computing SE amplitude, we assume that the nuclear magnetization in the volume dV corresponds to the mathematical and geometrical assumptions presented in Hahn's paper. For measuring, we set the second pulse q_2 so that $q_1 = q_2/2 = q$ and hence the flip angle is $\theta_1 = \theta_2/2 = \theta$. Under near resonance conditions and neglecting the relaxation and molecular diffusion, $M_\perp$ can be calculated as (Bloom, 1955)

$$M_\perp = -M_0 \sin(\theta_1) \times \sin^2(0.5\theta_2) = -M_0 \sin^3(\theta). \qquad (4)$$

Equation 1 resolves the water content in the subsurface $w(\mathbf{r})$. If we assume a horizontal stratification (1D case), equation 1 can be simplified to

$$e_0(q) = \int_z K(q,z)w(z)dz, \qquad (5)$$

where the kernel is

$$K(q,z) = \omega_0 \int_{x,y} \beta_1 \exp(j\varphi_0(\mathbf{r}))M_\perp(q)dxdy. \qquad (6)$$

The SE signal can be measured after attenuation by relaxation and molecular diffusion (Hahn, 1950). Technically, we cannot use a multi-echo technique, such as the one developed by Carr and Purcell (1954) for example, diffusion cannot be neglected. Thus, the SE signal at time $2\tau_e$ is

$$e_{2\tau_e} = e_0 \exp\left(-\frac{2\tau_e}{T_{2\mathrm{MRS}}}\right), \qquad (7)$$

with

$$\frac{1}{T_{2\mathrm{MRS}}} = \frac{1}{T_2} + \frac{D\gamma^2 G^2 \tau_e^2}{3}, \tag{8}$$

where $T_{2\mathrm{MRS}}$ is the observed relaxation time, G is the spatial magnetic field gradient, and D is the diffusion coefficient. Thus, when the diffusion is small, $T_{2\mathrm{MRS}}$ is an approximation of the T_2.

By making measurements with different values of τ_e we can estimate the time constant $T_{2\mathrm{MRS}}$ (Figure 1). Note that for resolving the water content using equation 5, the amplitude $e_{2\tau_e}$ has to be extrapolated using equation 7.

It should be noted that in the presence of the field gradient G, the envelope of echoes observed at different delays τ_{ei} is decaying faster than in homogeneous geomagnetic fields, which may cause some error in $T_{2\mathrm{MRS}}$ and consequently in the extrapolation. On the other hand, the diffusion effect depends on the absolute value of the gradient (Equation 8) and, in the geomagnetic field that is at least 1000-fold smaller than the field usually used for laboratory measurements, the diffusion effect may be relatively small (Shushakov and Fomenko, 2004); however, the diffusion effect on MRS measurements was never investigated and this subject requires a special study.

Inversion

Linear equation 5 can be approximated by a matrix equation (Legchenko and Shushakov, 1998). In matrix notation, equation 5 can be written as

$$\mathbf{Aw} = \mathbf{e_0}, \tag{9}$$

where $\mathbf{A} = [\tilde{a}_{n,j}] = \begin{bmatrix} \mathrm{Re}(a_{i,j}) \\ \mathrm{Im}(a_{i,j}) \end{bmatrix}$ is a rectangular matrix of $N \times J$ ($n = 1,2,\ldots,I,I+1,\ldots,N$; and $N = 2 \times I$) where the elements

$$\tilde{a}_{i,j} = \int_{z_j}^{z_{j+1}} K_j(q_i,z)dz, \tag{10}$$

$\mathbf{e_0} = (\tilde{e}_{01},\tilde{e}_{02},\ldots,\tilde{e}_{0n},\ldots,\tilde{e}_{0N})^T = (\mathrm{Re}(e_{01},e_{02},\ldots,e_{0i},\ldots,e_{0I}),\ \mathrm{Im}(e_{01},e_{02},\ldots,e_{0i},\ldots,e_{0I}))^T$ are the set of experimental data, $\mathbf{w} = (w_1,w_2,\ldots,w_j,\ldots,w_J)^T$ is the vertical distribution of water content, and the symbol T denotes transposition.

Different schemes can be used for resolving equation 9 (Guillen and Legchenko, 2002a; 2002b; Mohnke and Yaramanci, 2002; Braun et al., 2005). For this study, the inversion was carried out according to the well-known Tikhonov regularization method (Tikhonov and Arsenin, 1977).

MRS measuring scheme

A typical time diagram of MRS measuring is presented in Figure 1. Ambient noise is measured before current is transmitted in the loop. One pulse is sufficient for measuring the free induction decay signal (FID1) and the relaxation time T_2^*. Two pulses are necessary for measuring the relaxation time, and T_1, which is calculated using MRS signals FID1 and FID2, measured after the first and the second pulse, respectively. We can estimate T_1 by varying the delay between pulses (Legchenko et al., 2004). For measuring the spin echo (SE) signal, we also apply two pulses. The echo signal arrives after the second pulse at a time approximately equal to the time delay between the pulses (τ_e). Depending on the applied measuring scheme, it is possible to estimate the relaxation time T_{2MRS} by varying the time delay τ_e. Figure 1 shows three echo signals corresponding to different values of τ_e. For every fixed value of τ_e, only one echo can be measured.

An approximate shape of the envelope of an SE signal is given by Hahn (1950):

$$e_{SE}(t) = e_{2\tau_e} \exp\left(-\frac{(t-2\tau_e)^2}{2(T_2^*)^2} \right). \tag{11}$$

For practical use, it is convenient to present it as

$$e_{SE}(t) = e_{2\tau_e} \exp\left(-\frac{(t-2\tau_e)^2}{0.36\Delta t_{0.5}^2} \right), \tag{12}$$

where $\Delta t_{0.5}$ is the half-width of the echo signal (the width of the echo envelope at the level of one half of the maximum echo amplitude). Thus, the relaxation time T_2^* can be easily estimated as $T_2^* \approx 0.424 \times \Delta t_{0.5}$.

The SE amplitude could be estimated by fitting time records using equation 12; however, in practice such an approximation may result in an underestimate of the SE amplitude when the SE shape is different from the Gaussian.

RESULTS

Numerical modeling

Real experimental conditions of the MRS experiment may not obey the approximations that were made in our mathematical model, but still this model can be used for providing the first idea about MRS performance in the SE mode. The SE signal was computed using a simplified mathematical model (equations 1 and 4) and neglecting spin relaxation effects. For modeling, we use a square loop of 75 $\times$ 75 m^2, the Larmor frequency of 2000 Hz, the inclination of the geomagnetic field of 55°N and a half-space electrical resistivity of 50 ohm-m. FID1 and SE signals were computed assuming a 5-m-thick layer with 20% of the water content at different depths.

MRS measurements are carried out with a flip angle that varies within the investigated volume. Consequently, it follows from equations 1, 3, and 4 that the SE amplitude should be smaller than the FID signal amplitude. Results of numerical integration of equation 1 presented in Figure 2 show that for the same depth, the shapes of the sounding curves FID1 and SE are very similar, but the SE amplitude

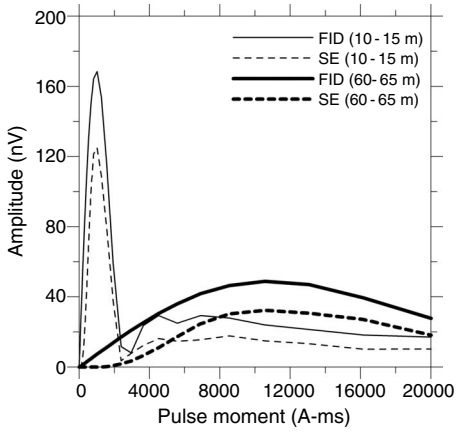

Figure 2. Example of FID1 and SE signals generated by a 5-m-thick water-saturated layer ($w = 20\%$) at different depths.

is about 25% smaller than the FID1 signal. Thus, we would expect that MR soundings in FID and SE modes would have similar characteristics; however, because the SE signal is smaller, we expect more difficulties when electromagnetic (EM) noise is present.

To estimate the depth of the investigation, we compute the MRS signal from a 1-m-thick layer of bulk water at different depths. Detection of this layer is possible if the signal is larger than the instrument threshold (10 nV for NUMIS system). In practice, the maximum pulse moment available with the NUMIS system for FID measurements is about 10,000 to 16,000 A-ms with a pulse duration of 40 ms. However, the SE signal has a larger frequency band than the FID signal and for this reason, pulses for applying the SE technique must be shorter than those for FID measurements. For modeling, we use two pulses, the first with a duration of 10 ms and a second with a duration of 20 ms, which make it possible to obtain the largest SE signal. Consequently, the maximum pulse moment would be about 2500 to 4000 A-ms. In Figure 3, the MRS amplitude from a 1-m-thick layer of bulk water ($w = 100\%$) is depicted against the layer depth. The signal was calculated considering the maximum pulse moment of 10,000 A-ms for an FID signal and 4000 A-ms for an SE signal. Under noiseless conditions, the depth of investigation is about 100 m in FID mode and 60 m in SE mode. It should be noted that even if we were able to produce equal pulses for the FID and SE measurements (10,000 A-ms, for example), the SE signal would be smaller than the FID signal and consequently the depth of investigation would also be smaller (about 80 m).

Vertical resolution of the MRS method depends on the kernel of the integral equation 1 and the signal-to-noise ratio (Twomey, 1974). Because the kernel for the FID and SE measurements is not the same, we expect that resolution with the same S/N may also be different. For comparison, we compute the eigenvalues for the three examples discussed above. The results are presented in Figure 4. Each eigenvalue j of the matrix $\mathbf{A}$ (equation 4) corresponds to one theoretical layer at depth j. Layers with larger eigenvalues can be better resolved. For the MRS inverse problem, smaller eigenvalues of the matrix $\mathbf{A}$ correspond to deeper layers (Legchenko and Shushakov, 1998). It can be seen in Figure 4 that for the same value of the maximum pulse moment, the FID and SE soundings will have about equal resolution down to the depth corresponding to the 10th eigenvalue, which corresponds to approximately 60 m. For greater depth, the SE sounding should have slightly better resolution than the FID sounding. However, as the maximum available pulse moment for SE measurements is always smaller than for FID measurements, the MRS resolution in the SE mode will be worse than in FID mode.

Experimental results

Magnetic resonance soundings using the SE technique were performed in Cyprus in 1999. The study area was an aquifer composed of coarse sand and gravel that are alteration products of limestone (white grains) and basalt (black grains). Measurements of the magnetic susceptibility of the rock samples revealed values of about 10^{-2} SI units for basalt material and 10^{-4} to 10^{-5} SIU for limestone material. Measurements of the geomagnetic field at the surface confirmed the heterogeneity of the earth's field as a result of the presence of basalt. In 2008, we used MRS in the SE mode in Canada to investigate aquifers composed of fine to medium sand containing 1% to 2% magnetite grains. The perturbation of the magnetic resonance signal caused by this mineral was studied in the laboratory by Hirasaki and Roy in 2004 (Roy et al., 2008). In 2008, SE measurements were also conducted in southern India. The aquifer under study was about 20 m thick and was composed of quartz sand with a magnetic susceptibility of less than 10^{-4} SIU, which usually has no effect on MRS measurements. However, this sand overlies a gneissic basement with a magnetic susceptibility of about 10^{-2} SIU. Moreover, a geological feature (probably a dike into the gneissic bedrock) creates a geomagnetic field gradient of about 1000 nT over a distance of about 200 m at the surface. We have observed that such a gradient has an effect on the MRS signal.

For MRS measurements, we used several modifications of the NUMIS instrument developed by IRIS Instruments (France): NUMIS (in Cyprus), NUMIS^{PLUS} (in India,) and NUMIS^{LITE} (in Canada).

Figure 5 shows examples of the SE records at different sites. The time interval τ_e is measured between the centers of the pulses. In Cyprus, we observe a Gaussian-shape SE signal shifted in time from the second pulse (Figure 5a, see also Figure 1). Normally the echo signal should be centered at time τ_e from the second pulse. However, as we use relatively long pulses (approximately 10 and 20 ms) with nonideal rectangular shapes, the echo arrives about 15 to 20 ms earlier. The fact that the signal shift is fully controlled by τ_e confirms that we are really observing the SE signal. Because the relaxation time T_{2MRS} is long (about 1100 ms), we do not observe a decrease of the SE am-

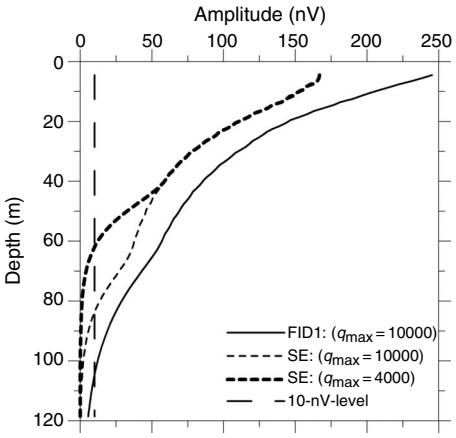

Figure 3. Amplitudes generated by a 1-m-thick layer of bulk water versus the layer depth considering $q_{max} = 10000$ A-ms and $q_{max} = 4000$ A-ms pulse moments.

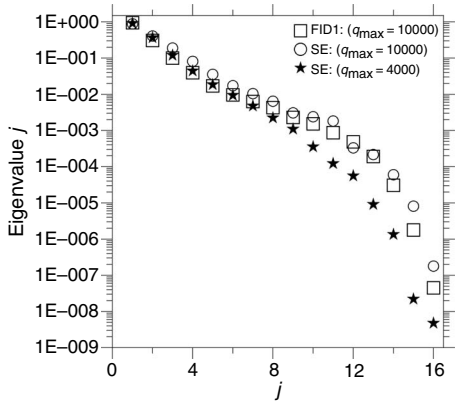

Figure 4. Normalized eigenvalues of the matrix $\mathbf{A}$ computed for FID1 and SE inversions considering $q_{max} = 10000$ A-ms and $q_{max} = 4000$ A-ms pulse moments.

plitude with increasing value of τ_e. In India (Figure 5b), τ_e was set much longer and we observed the relaxation of the SE signal. Because the heterogeneity of the geomagnetic field in India was smaller than in Cyprus, the FID signal was also observed immediately after the second pulse. In Canada, a lower percentage of magnetite in the sand (St. Marthe location in Figure 5d as compared to the St. Fulgence location in Figure 5c) corresponds to a wider SE signal. This is also why at the St. Marthe location we observed both SE and FID signals. A summary of our field observations is presented in Table 1.

The SE amplitude can be computed using equation 4 if the local distribution of the Larmor frequencies is symmetrical (Hahn, 1950). In order to verify the applicability of this assumption to MRS, we measured the spectra of SE signals (Figure 6). In India (Figure 6a) and at St. Fulgence, Canada (Figure 6b), we observed approximately symmetrical spectra; however at Maniwaki, Canada (Figure 6c), the shapes of the observed spectra are more complicated. The corresponding examples of SE records are presented in Figure 7. For each measurement, the SE envelope was approximated by a Gaussian function using equation 12. For fitting, we used the algorithm proposed by Legchenko and Valla (1998) using the Gaussian fit instead of the exponential fit. We observe that signals measured in India (Figure 7a) and at St. Fulgence (Figure 7b) have a shape similar to the Gaussian. At Maniwaki, the SE envelope is less regular and the Gaussian approximation provides an estimate of the SE amplitude but does not make it possible to describe all signal details.

Plotting the amplitudes of the SE signal versus two times the delay between pulses makes it possible to estimate the T_{2MRS} relaxation time (Figure 8). In Figure 8, the measured SE signal is well fitted by an exponential function but due to the limited accuracy of MRS data and unknown diffusion rate, it is not possible to measure T_{2MRS} with a high accuracy. Errors in the estimate of T_{2MRS} may cause nonnegligible errors in extrapolation and consequently in estimated water content.

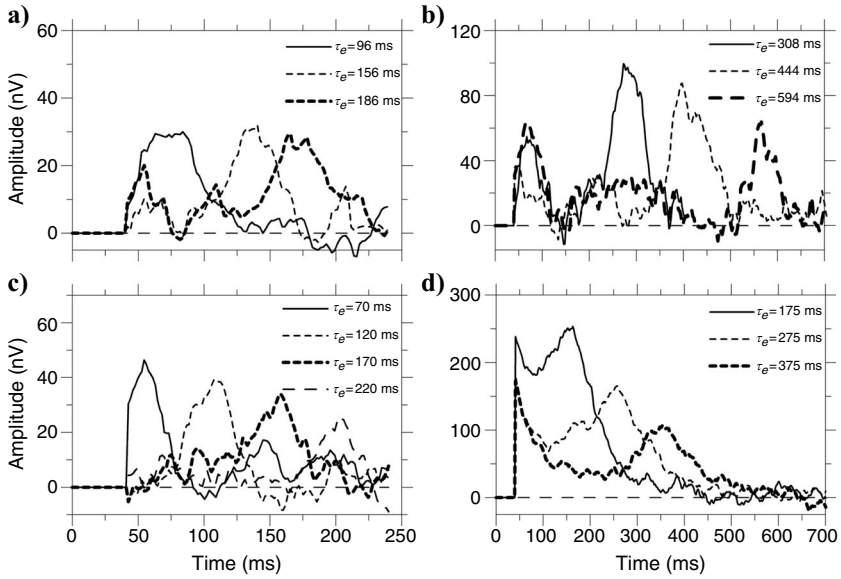

Figure 5. Example of SE records: (a) Cyprus (Phafos, July 1999); (b) India (P3-sea, November 2008); (c) Canada (St. Fulgence, August 2008); (d) Canada (St. Marthe, August 2008). Time zero corresponds to the end of the second pulse.

Table 1. Overview of MRS results.

Site	Loop	e_{FID}	FID: T_2^* (ms)	τ_e (ms)	$e_{2\tau_e}$ (nV)	$\Delta t_{0.5}$ (ms)	SE: T_2^* (ms)	T_{2MRS} (ms)	Rock type
St. Fulgence, Canada	Eight 19 m, 2 turns	0	—	70	65	35	15	444	Sand with magnetite
St. Marthe, Canada	Eight 37.5 m, 1 turn	200	90	175	250	205	87	420	Sand with magnetite
Maniwaki, Canada	Eight 37.5 m, 1 turn	0	—	70	157	85	36	264	Medium to coarse sand with magnetite
P1-sea, India	Square 50 m, 2 turns	500	165	620	80	380	160	950	Coarse sand overlying magnetic basement
P3-sea, India	Square 50 m, 2 turns	90	Var: 600-70	594	65	155	49	750	Coarse sand overlying magnetic basement
Phafos, Cyprus	Square 75 m, 1 turn	0	—	96	40	45	20	1100	Coarse sand and gravel with a basalt component

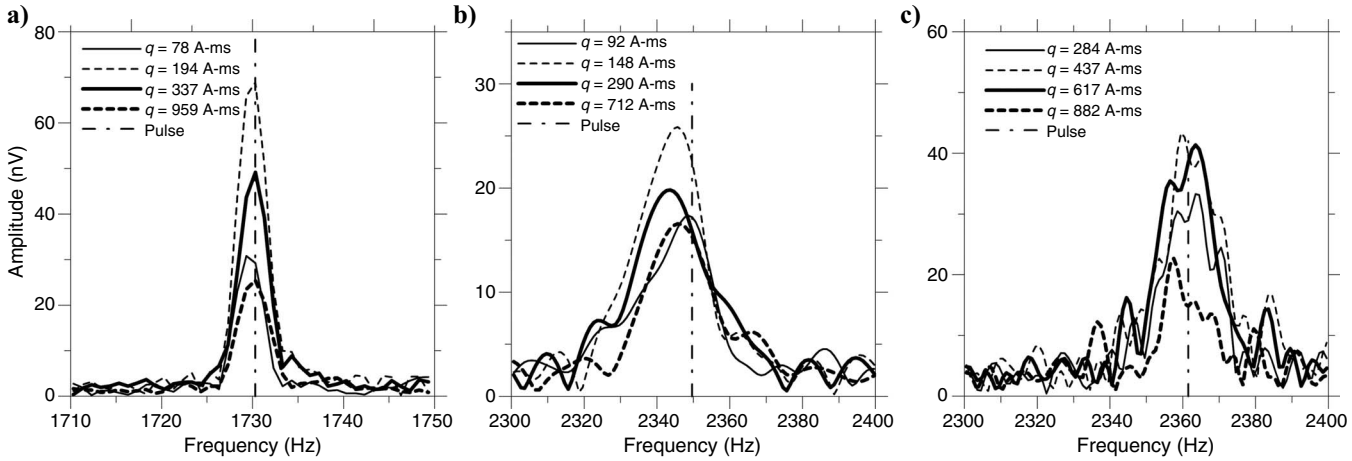

Figure 6. Example of SE spectra corresponding to different pulse moments: (a) P1-sea, India; (b) St. Fulgence, Canada; (c) Maniwaki, Canada.

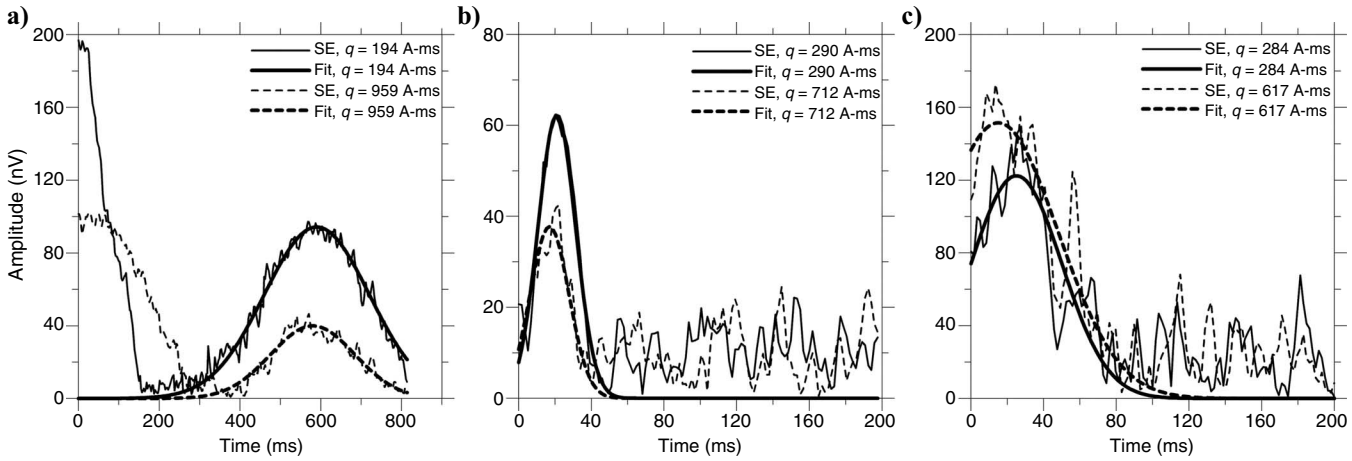

Figure 7. Example of SE signals and their fit corresponding to different pulse moments: (a) P1-sea, India; (b) St. Fulgence, Canada; (c) Maniwaki, Canada.

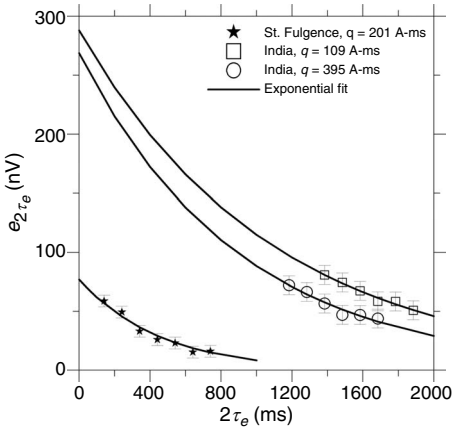

Figure 8. Example of SE amplitude versus delay between the pulses and their exponential fit in Canada (St. Fulgence) and in India (P1-sea, two different pulse moments).

We investigated T_2 measurements for arbitrary flip angles in India. Time-domain electromagnetic measurements (TDEM) and geologic data suggest that the aquifer is homogeneous down to about 20 m, and we measured $T_{2\mathrm{MRS}}$ and T_2^* versus the pulse moment (Figure 9a). We observe that within the investigated aquifer, $T_{2\mathrm{MRS}}$ is approximately stable, which confirms the possibility of measuring T_2 with MRS. FID and SE measurements of T_2^* in the shallow part of the aquifer show similar values but results are different for larger pulse moments. We explain this effect as a result of the basement influence being stronger in the deeper part of the aquifer. Results of T_2^* measurements in Canada (Figure 9b) show relatively uniform values for all pulse moments. The observed dispersion of the measurements is due to limited accuracy of MRS when measuring short signals.

When SE spectra are symmetrical, the 180° phase shift of the second pulse should not cause changes in the SE amplitude (Equation 4). In order to verify the symmetry assumption, we have compared the SE signals using the $(q, -2q)$ and $(q, 2q)$ measuring sequences at the same location and using the same loop. The results are presented in Figure 10. We do not observe much difference between measurements with the $(q, 2q)$ and $(q, -2q)$ sequences at St. Fulgence (Figure 10a). At Maniwaki, however, the difference is the largest observed during our field work (Figure 10b). We have no explanation for this result. Assuming that it is not an instrumental error, we might suggest that the subsurface has a more complicated structure and that the echo formation conditions do not fully correspond to the assumptions made by Bloom.

Figures 11 and 12 present a comparison of MRS results in SE mode with a borehole at Miniwaki, Canada. Attempts to measure the FID signal were not successful, thus confirming results reported by Roy et al. (2008). We measured both SE signals using the $(q, -2q)$ and $(q, 2q)$ sequences. The aquifer investigated by borehole PP-1 is composed of medium to coarse sand (Roy et al., 2008). MRS inversions were carried out using the smooth inversion algorithm and complex signals (Figure 11a). The depth of investigation was estimated as approximately 15 m (Figure 11b). For both data sets, the inversion results correspond well to the borehole log. The water content of 25%–35% is in general agreement with the porosity expected for sand. Observed differences between the water content obtained with $(q, -2q)$ and $(q, 2q)$ sequences are due to the difference in SE amplitude, probably caused by nonsymmetrical spectra of SE signals and thus demonstrate the uncertainty in MRS results. However, SE results compare more favorably with FID measurements that showed a zero-signal. Figure 12 shows that the two different models provided by the inversion fit well with our experimental data (both amplitude and phase).

Figures 13 and 14 show the comparison of MRS results in FID and SE mode obtained in India. This site is located at a distance of about 500 m from the magnetic anomaly, and the FID signal does not seem to be perturbed; however, the gneissic basement probably also perturbs the geomagnetic field, thus creating a small heterogeneity sufficient for measuring the SE signal. The vertical distribution of the MRS water content (Figure 13a) shows that the water level was about 2 m deep, which was in agreement with the ground truth. The FID and SE inversions both show a water content of about 30%–40% with more water close to the surface. Measurements of the porosity of the sand samples in the laboratory ranged from 26% to 36%. Moreover, the MRS results are in agreement with TDEM (Figure 13b). The resistivity log discriminates three layers: the shallow low-conductivity layer corresponds to a fresh water aquifer, the high conductivity layer shows a saline water aquifer, and a deep low conductivity layer represents the basement. The maximum depth of detection for a 1-m-thick layer of bulk water is estimated to be about 16–18 m for SE measurements and a bit more than 30 m for FID measurements (Figure 13c). We can consider this estimate as the maximum depth of investigation for this sounding setup. Figure 14 shows the measured amplitude and phase of the FID and SE signals and the theoretical signal reconstructed after inversion results. Both FID and SE inversions show a reasonable fit with experimental data.

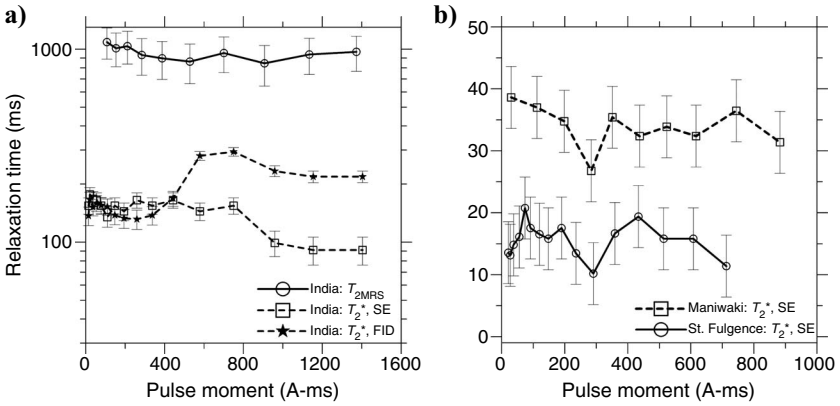

Figure 9. Example of the relaxation time versus the pulse moment: (a) P1-sea, India (T_2^* measured with SE and FID and T_{2MRS} measured with SE); (b) Maniwaki and St. Fulgence, Canada (T_2^* measured with SE).

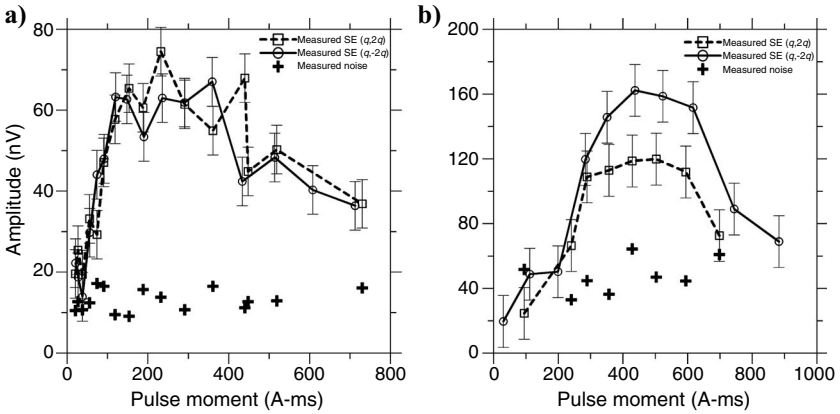

Figure 10. Comparison of the $(q, 2q)$ and $(q, -2q)$ SE signals: (a) 19-m-loop (St. Fulgence, Canada); (b) 37 − 5-m-loop (Maniwaki, Canada).

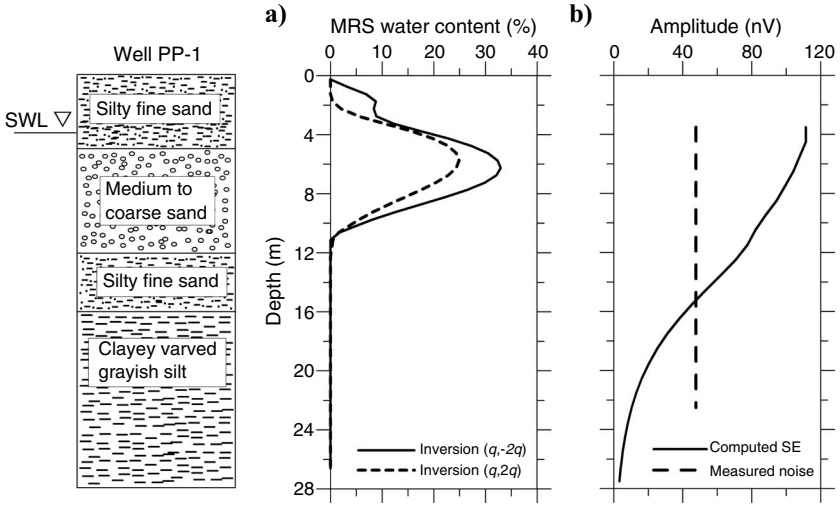

Figure 11. Example of inversion results (test site: Maniwaki, Canada): (a) borehole geological description and water content versus depth (solid line — inversion of $(q, -2q)$ data, dashed line — inversion of $(q, 2q)$ data); (b) amplitude of 1-m-thick layer of bulk water versus depth (solid line) and average noise level for this site (dashed line).

DISCUSSION

We have tested the MRS method in SE mode under different geological conditions in confirmed heterogeneous geomagnetic fields: a coarse sand and gravel aquifer containing basalt gravel, a sand aquifer containing 1%–2% of magnetite, and a coarse sand aquifer over a gneissic basement with a magnetic dike. In all three test sites, we were able to observe a magnetic resonance response. We observed only the SE signal in some cases and both the FID and SE signals in others. Thus, depending on the heterogeneity of the geomagnetic field, there are three possibilities: in homogeneous geomagnetic fields (limestone, chalk), we can measure the FID signal but not the SE signal; in nonhomogeneous geomagnetic fields (sand with magnetic particles), we can measure the SE signal but not the FID signal; and under transitional conditions characterized by relatively small perturbations of the geomagnetic field, we can measure both the FID and SE signals.

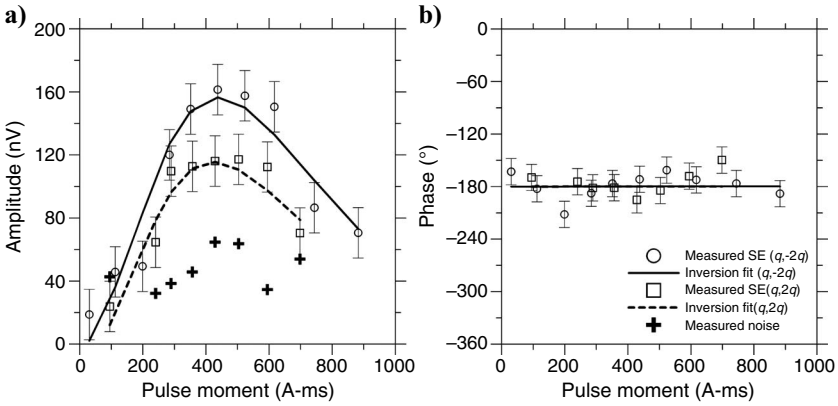

Figure 12. Measured SE (a) amplitude and (b) phase and corresponding inversion fit versus pulse parameter (test site: Maniwaki, Canada) for $(q, -2q)$ and $(q, 2q)$ data sets.

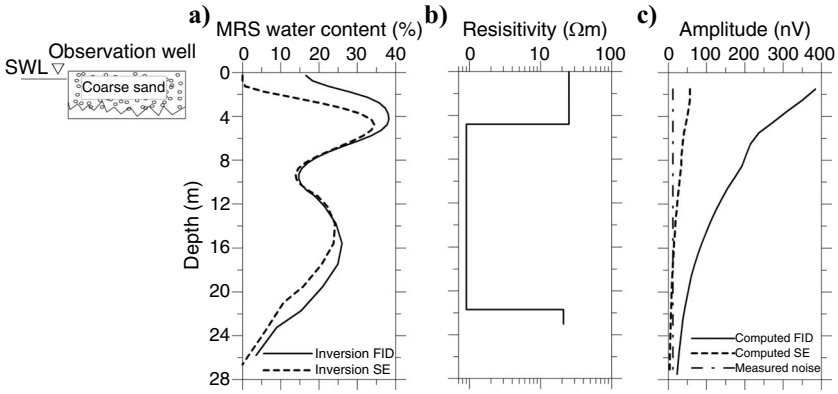

Figure 13. Example of inversion results (test site: P1-sea, India): (a) water content versus depth (solid line — FID inversion, dashed line — SE inversion); (b) resistivity log given by TDEM measurements; (c) amplitude of 1-m-thick layer of bulk water versus depth (solid line) and average noise level for this site (dashed line).

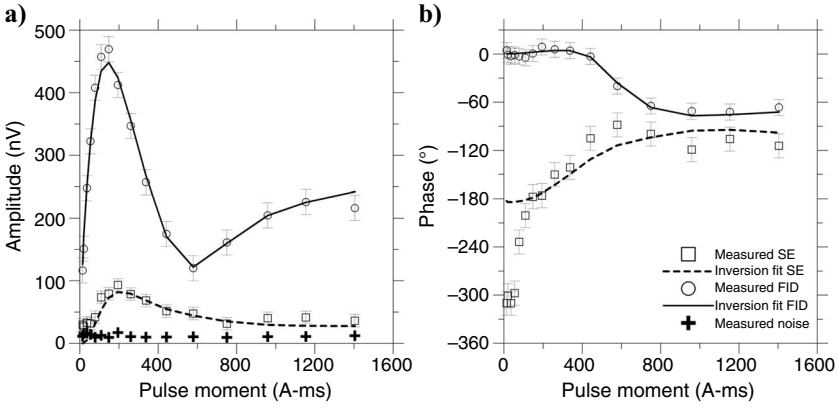

Figure 14. Measured FID and SE (a) amplitude and (b) phase and corresponding inversion fit versus pulse parameter (test site: P1-sea, India).

Numerical modeling reveals that MRS in SE mode is less efficient than the FID technique currently used: the SE signal is smaller; the wider band of the SE signal makes it necessary to apply the amplifier with a relatively wide band, which diminishes the signal-to-noise ratio; and SE measurements require a wider band of excitation pulses and consequently a more powerful current generator. If we were not limited by the power of the current pulse, the vertical resolution of MRS in SE mode would be similar to that of the FID mode (for equal signal-to-noise ratio). However, in practice, the power limitation reduces the resolution of MRS when the SE signal is measured. For our study, we used a simplified mathematical model and many details typical for real measurements have been omitted. The development of a more sophisticated model is a matter of further research, but we believe the simplified model gives us an idea of the performance of the SE method applied to MRS measurements.

While investigating an aquifer in India, we found FID and SE results in agreement with TDEM and porosity measurements of laboratory sand samples. We estimated T_{2MRS} as 950 ms in water-saturated sand. Taking into account that in bulk water T_2 is about 2000 ms, we do not expect that in India the diffusion was large. This demonstrates that under India conditions, our field procedure and interpretation software are sufficiently accurate. We are not able to estimate the diffusion effect on our results in Canada and hence the MRS estimate of the water content in Canada should be considered as a qualitative result. Thus, MRS-SE performance is site dependent and the effect of diffusion on MRS results requires investigation. One of the possible ways to diminish the diffusion effect on the estimation of the water content consists of reducing the minimum available delay between the pulses, thus reducing the extrapolation length.

We tested the traditional SE technique using a $(q, 2q)$ pulse sequence and compared it to the SE measured with the 180° phase shift of the second pulse denoted as a $(q, -2q)$ pulse sequence. Re-

sults show that in both cases, the signal can be measured but the amplitude is not always equal for the two types of measurement, which contradicts the ideal system described by Bloom's equations. Inversion of these two data sets (Figure 11a) shows that the uncertainty caused by the nonideality of the spin system returns an estimate of the water content 25% and 33% for $(q, 2q)$ and $(q, -2q)$ data sets, respectively. Hydrogeologists estimate the sand porosity of this aquifer at approximately 30%. Thus, SE results show a water content much closer to the expected value than the FID-derived water content, which shows an obviously erroneous value (0%) for the water-saturated sand. We observed that the difference between $(q, 2q)$ and $(q, -2q)$ measurements was the largest at Maniwaki, where the relaxation time T_2 was relatively short and processes on the grain surface probably have a greater effect on the SE measurements. We did not observe any correlation between the frequency offset during measuring and the observed difference between $(q, 2q)$ and $(q, -2q)$ measurements. A complete understanding of this phenomenon requires a more detailed study.

CONCLUSIONS

We developed and successfully tested a methodology to apply the MRS method to the investigation of aquifers containing magnetic materials. Where the FID method fails or produces erroneous results, the MRS-SE method can produce useful results. We have shown this for several sites on three different continents and in different geological scenarios. Considering the widespread occurrence of magnetic rocks, this development significantly increases the area of application of MRS; however, even if the first results are promising, we need additional experience in quantitatively evaluating the SE technique applied to MRS.

Assuming the ideal conditions formulated by Bloom, we developed a simplified mathematical model that makes it possible to model and interpret SE measurements. Our numerical results show that the MRS method in the SE mode is less efficient than the FID technique because of the smaller amplitude and wider band of the SE signal. An estimate of the water content with the SE requires longer extrapolation time than FID measurements; hence, the SE method is quite sensitive to errors in measuring the relaxation time T_2 and the diffusion influence on the T_2 estimate. Consequently, for an accurate and site-independent estimation of the water content, detailed investigation of the diffusion effect on MRS-SE results under different experimental conditions is necessary. One of the possible ways to diminish the diffusion effect on the estimation of the water content consists of reducing the minimum available delay between the pulses. This approach will require corresponding instrumental developments.

Due to instrumental limitations, unknown diffusion rate, and unknown distribution of the magnetic fields within investigated volume (which limits the accuracy of the mathematical model), performance of the presented MRS-SE approach is site dependent. In a general case, MRS-SE in its current implementation is not able to provide robust estimates of the initial amplitude; therefore, for accurate estimate of the water content, more sophisticated approaches need to be developed.

ACKNOWLEDGMENTS

The authors are thankful to L. Nandagiri from National Institute of Technology of Karnataka, (India); Alain Rouleau from UQAC (Chicoutimi, Québec); Michel Chouteau from Ecole Polytechnique (Montreal, Québec;) and Michel Bureau from MBG (Brossard, Québec) for their help in organizing field experiments. We thank Tamas Nemeth, Lev Eppelbaum, and four anonymous reviewers for their comments and suggestions which helped improve the manuscript.

The results presented were obtained within the framework of the French national research projects FNS WATERSCAN and ANR REMAPRO. Field experiments in Canada and India were supported by research funds from the BRGM (France), the Action Contre la Faim, and the French Red Cross nongovernmental organizations.

REFERENCES

Bloom, A. L., 1955, Nuclear induction in inhomogeneous fields: Physical Review, **98**, no. 4, 1105–1111, doi: 10.1103/PhysRev.98.1105.

Braun, M., M. Hertrich, U. Yaramanci, 2005, Study on complex inversion of magnetic resonance sounding signals: Near Surface Geophysics, **3**, 155–163.

Carr, H. Y., and E. M. Purcell, 1954, Effects of diffusion on free precession in nuclear magnetic experiments: Physical Review, **94**, no. 3, 630–638, doi: 10.1103/PhysRev.94.630.

Guillen, A., and A. Legchenko, 2002a, Application of linear programming techniques to the inversion of proton magnetic resonance measurements for water prospecting from the surface: Journal of Applied Geophysics, **50**, no. 1–2, 149–162, doi: 10.1016/S0926-9851(02)00136-2.

Guillen, A., and A. Legchenko, 2002b, Inversion of surface nuclear magnetic resonance data by an adapted Monte-Carlo method applied to water resource characterization: Journal of Applied Geophysics, **50**, no. 1–2, 193–205, doi: 10.1016/S0926-9851(02)00139-8.

Hahn, E. L., 1950, Spin echoes: Physical Review, **80**, no. 4, 580–594, doi: 10.1103/PhysRev.80.580.

Legchenko, A., J.-M. Baltassat, A. Beauce, and J. Bernard, 2002, Nuclear magnetic resonance as a geophysical tool for hydrogeologists: Journal of Applied Geophysics, **50**, no. 1–2, 21–46, doi: 10.1016/S0926-9851(02)00128-3.

Legchenko, A., J.-M. Baltassat, A. Bobachev, C. Martin, H. Robain, and J.-M. Vouillamoz, 2004, Magnetic resonance sounding applied to aquifer characterization: Journal of Ground Water, **42**, no. 3, 363–373, doi: 10.1111/j.1745-6584.2004.tb02684.x

Legchenko, A., M. Ezersky, J.-F. Girard, J.-M. Baltassat, M. Boucher, C. Camerlynck, and A. Al-Zoubi, 2008, Interpretation of magnetic resonance soundings in rocks with high electrical conductivity: Journal of Applied Geophysics, **66**, no. 3–4, 118–127, doi: 10.1016/j.jappgeo.2008.04.002.

Legchenko, A. V., and O. A. Shushakov, 1998, Inversion of surface NMR data: Geophysics, **63**, 75–84, doi: 10.1190/1.1444329.

Legchenko, A., and P. Valla, 1998, Processing of surface proton magnetic resonance signals using non-linear fitting: Journal of Applied Geophysics, **39**, no. 2, 77–83, doi: 10.1016/S0926-9851(98)00011-1.

Legchenko, A., and P. Valla, 2002, A review of the basic principles for proton magnetic resonance sounding measurements: Journal of Applied Geophysics, **50**, no. 1–2, 3–19, doi: 10.1016/S0926-9851(02)00127-1.

Mohnke, O., and U. Yaramanci, 2002, Smooth and block inversion of surface NMR amplitudes and decay times using simulated annealing: Journal of Applied Geophysics, **50**, no. 1–2, 163–177, doi: 10.1016/S0926-9851(02)00137-4.

Roy, J., A. Rouleau, M. Chouteau, and M. Bureau, 2008, Widespread occurrence of aquifers currently undetectable with the MRS technique in the Grenville geological province, Canada: Journal of Applied Geophysics, **66**, no. 3–4, 82–93, doi: 10.1016/j.jappgeo.2008.04.006.

Shushakov, O. A., 1996, Surface NMR measurement of proton relaxation times in medium to coarse-grained sand aquifer: Magnetic Resonance Imaging, **14**, no. 7–8, 959–960, doi: 10.1016/S0730-725X(96)00194-4.PubMed

Shushakov, O. A., and V. M. Fomenko, 2004, Surface-NMR relaxation and echo of aquifers in geomagnetic field: Applied Magnetic Resonance, **25**, no. 3–4, 599–610, doi: 10.1007/BF03166551.

Slichter, C. P., 1990, Principles of magnetic resonance, 3rd edition: Springer-Verlag, Berlin Heidelberg.

Tikhonov, A., and V. Arsenin, 1977, Solution of ill-posed problems: John Wiley & Sons, Inc.

Twomey, S., 1974, Information content in remote sensing: Applied Optics,

13, no. 4, 942–945.
Valla, P., and A. Legchenko, 2002, One-dimensional modelling for proton magnetic resonance sounding measurements over an electrically conductive medium: Journal of Applied Geophysics, **50**, no. 1–2, 217–229, doi: 10.1016/S0926-9851(02)00141-6.
Weichman, P. B., E. M. Lavely, and M. H. Ritzwoller, 2000, Theory of surface nuclear magnetic resonance with applications to geophysical imaging problems: Physical Review E: Statistical Physics, Plasmas, Fluids, and Related Interdisciplinary Topics, **62**, no. 1, 1 Pt B, 1290–1312, doi: 10.1103/PhysRevE.62.1290.